



**HAL**  
open science

# Universal scaling laws in turbulent Rayleigh-Bénard convection with and without roughness

Lyse Brichet, Romane Braun, Lucas Méthivier, Elian Bernard, Francesca Chillà, Julien Salort

► **To cite this version:**

Lyse Brichet, Romane Braun, Lucas Méthivier, Elian Bernard, Francesca Chillà, et al.. Universal scaling laws in turbulent Rayleigh-Bénard convection with and without roughness. 2024. hal-04434081

**HAL Id: hal-04434081**

**<https://hal.science/hal-04434081>**

Preprint submitted on 2 Feb 2024

**HAL** is a multi-disciplinary open access archive for the deposit and dissemination of scientific research documents, whether they are published or not. The documents may come from teaching and research institutions in France or abroad, or from public or private research centers.

L'archive ouverte pluridisciplinaire **HAL**, est destinée au dépôt et à la diffusion de documents scientifiques de niveau recherche, publiés ou non, émanant des établissements d'enseignement et de recherche français ou étrangers, des laboratoires publics ou privés.

# Universal scaling laws in turbulent Rayleigh-Bénard convection with and without roughness

Lyse Brichet, Romane Braun, Lucas Méthivier, Elian Bernard, Francesca Chillà, and Julien Salort\*

*ENSL, CNRS, Laboratoire de physique, F-69342 Lyon, France.*

(Dated: February 1, 2024)

Experimental measurements of heat-flux and velocity in turbulent Rayleigh-Bénard convection are reported on a wide range of operating conditions, with either smooth or rough boundaries, in water or fluorocarbon, and aspect ratios 1 or 2. The heat-flux, expressed as the dimensionless parameter Nusselt number is found in agreement with Grossmann-Lohse prediction in smooth cells. The new measurements in the rough cell with fluorocarbon, which reaches Rayleigh numbers,  $Ra$ , up to  $2.5 \times 10^{12}$  at  $Pr = 11$ , the Nusselt number show a clear  $Ra^{1/2}$  scaling, hinting a fully turbulent regime. The  $Nu$  vs  $Ra$  relationship is not unique, in that it depends on the cell geometry, plate roughness, Prandtl numbers, as well as details in the experimental setup. The Reynolds number essentially scales like  $Re \propto Ra^{1/2} Pr^{-0.7}$  for all experiments, but show deviations with the various flow configurations. We find that the dimensionless heat-flux, expressed as  $RaNu$ , has a universal scaling with Reynolds number, collapsing all data, rough or smooth, even those in the literature where the  $Nu$  vs  $Ra$  scaling is in apparent contradiction.

Turbulent Rayleigh-Bénard Convection (RBC) is a model system where a layer of fluid is heated from below and cooled from above. It is controlled by three dimensionless parameters: the Rayleigh number  $Ra$ ,

$$Ra = \frac{g\alpha\Delta TH^3}{\nu\kappa}, \quad (1)$$

the Prandtl number  $Pr$ ,

$$Pr = \frac{\nu}{\kappa}, \quad (2)$$

and the aspect ratio  $\Gamma = L/H$ , where  $g$  is the acceleration of gravity,  $\alpha$  the thermal expansion coefficient,  $\Delta T$  the temperature difference across the fluid layer,  $\nu$  the kinematic viscosity,  $\kappa$  the thermal diffusivity,  $H$  the height of the cell, and  $L$  the width of the cell. A long standing endeavour consists in finding universal scaling laws for the heat transfer, expressed as the dimensionless parameter Nusselt number  $Nu$  [1, 2],

$$Nu = \frac{\dot{q}H}{\lambda\Delta T}, \quad (3)$$

where  $\dot{q}$  is the heat-flux, and  $\lambda$  the thermal conductivity. This would allow extrapolating results from laboratory experiments to natural systems where highly turbulent natural convection plays a role. These include in particular convection in the ocean at the pole or in subglacial lakes [3], resulting in Rayleigh numbers beyond  $10^{14}$ , and to the “ultimate regime” of convection where  $Nu \sim Ra^{1/2}$  (with logarithmic corrections) [4]. However, experimental heat-transfer measurements published in the literature for  $Ra > 10^{11}$  seem to be contradictory, some showing a transition at  $Ra \approx 10^{11}$  [5, 6], some showing a delayed transition at higher  $Ra$  [7], or no transition at all [8]. These experiments are within Oberbeck-Boussinesq conditions [9] and share similar geometries, but differ in Prandtl numbers and details in

the setup. It now seems clear that the transition to the ultimate regime may be a subcritical process, and may depend on aspect ratio and Prandtl numbers [10–12].

In this letter, we evidence a way to recover universality. We report new velocity data obtained from shadowgraph imaging in parallelepiped Rayleigh-Bénard cells with or without roughness and using either deionised water or Fluorocarbon FC-770 as the working fluid. The cell dimensions are 41.5 cm  $\times$  41.5 cm  $\times$  10.5 cm for the aspect ratio 1 cell, and 20 cm  $\times$  41.5 cm  $\times$  10.5 cm for the aspect ratio 2 cell. The details of the cell are described in [13]. The Rayleigh number spans a wide range between  $10^9$  and  $2.5 \times 10^{12}$ , the Prandtl number between 4.3 and 7.0 in water, and 11 and 14 in FC-770, and the aspect ratio 1 or 2. In these conditions, the flow can be quite different, the scaling exponent of  $Nu$  versus  $Ra$  also quite different, and in apparent disagreement with data from Grenoble, Oregon and Göttingen cited above. And yet, all the data can be collapsed using the appropriate scaling of Reynolds and Prandtl numbers.

The cells can be set up with roughness on the bottom plate, consisting in square roughness elements of height  $h_0 = 2$  mm, machined in the plate, as described in [14]. In that case, the cell (later referred to as “RS”), is asymmetrical, with a rough bottom plate, and a smooth top plate. As shown in our previous works [15, 16], this allows to define Rayleigh and Nusselt numbers of the rough and smooth halves. The smooth cell (later referred to as “SS”) has entirely smooth boundaries, as described in [13]. We have now operated the rough configuration (RS) with Fluorocarbon FC-770 thus significantly extending the previous heat-transfer results in water [17], see Figure 1. In the Fluorocarbon cell, the thermal boundary layer, estimated as  $\delta_{th} = H/(2Nu)$ , ranges between 250  $\mu$ m and 500  $\mu$ m, much smaller than the roughness height  $h_0$ . The kinetic boundary layer, estimated as  $\delta_v \approx \delta_{th} Pr^{1/3}$  ranges between 600  $\mu$ m and 1100  $\mu$ m,

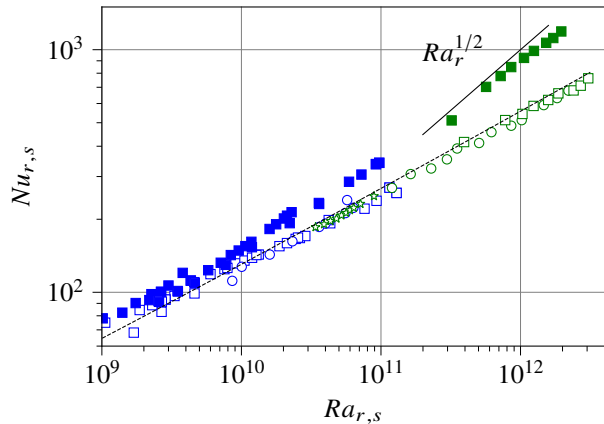


FIG. 1. Heat-transfer measurements. Blue: deionized water. Green: Fluorocarbon FC-770. Full squares: rough half-cell of RS cell. Open squares: smooth half-cell of RS cell. Circles: SS cell. Stars: SS cell with  $\Gamma = 2$ . RS cell in water from [17]. SS cells in FC-770 from [13]. SS cell in water and RS cell in FC-770: new data. Solid black line:  $Ra^{1/2}$ . Dashed black line: Grossmann-Lohse model [2]

smaller than the roughness height  $h_0$ . Therefore, the rough cell lies in Regime III as defined by Xie & Xia [18]. While the rough half-cell has a  $Ra^{1/2}$  scaling, the smooth half-cell is in good agreement, over more than 3 decades of Rayleigh numbers, with heat-transfer measurements in SS cell, as well as with the Grossmann-Lohse model [2]. This shows that the top and bottom plates remain independent, even very far from the roughness-triggered enhancement threshold, and holds even when the Nusselt number of the bottom half is nearly twice as large as that of the top half. This is a major result that shows how the boundary layers adapt themselves to maintain the heat-flux constant.

We computed the velocity fields using *Correlation Image Velocimetry* on shadowgraph recordings for all of them, yielding consistent estimates for both the mean and fluctuation velocities, as well as consistent Reynolds number estimates in all configurations. The method has previously been validated against *Particle Image Velocimetry* in experimental conditions where both were possible [13]. While we find that the mean flow has the same structure at  $Ra = 10^9$  and  $Ra = 10^{12}$ , the velocity fluctuations differ, see Figure 2. At higher Rayleigh numbers, and in this range of Prandtl where we do not see evidence for a transition to the ultimate regime, we find that the velocity fluctuations are globally much larger, and also more focused near the impinging jets than in the lower Rayleigh number case.

When roughness is added to the bottom plate, mean velocity is increased between 5% and 20% in the range of parameters explored in this work, but the overall structure of the mean flow is not significantly changed, see Figure 3. We focus on the velocity of the upwelling and

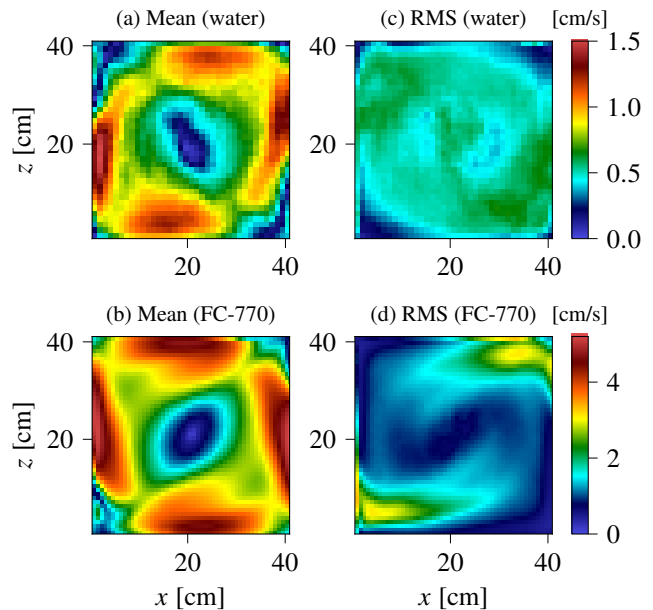


FIG. 2. Mean (a, b) and RMS (c, d) velocity maps computed from the Shadowgraph recording. (a, c) Water  $Ra = 2.3 \times 10^{10}$ ,  $Re = 5.4 \times 10^3$ ,  $v_{\max} = 1.5$  cm/s; (b, d) FC-770  $Ra = 1.7 \times 10^{12}$ ,  $Re = 3.3 \times 10^4$ ,  $v_{\max} = 5.2$  cm/s.

downwelling jets to allow comparison with the literature where velocity is estimated with pairs of thermometers at mid-height [19–21]. In symmetrical cells, we average the velocity of the downwelling and upwelling jets. In RS cells, we associate the downwelling jet with the top plate, and the upwelling jet with the bottom plate. Indeed, we use the following definition for the Reynolds numbers,  $Re_{r,s}$  of the rough bottom and the smooth top,

$$Re_{r,s} = \frac{U_{\text{up,down}} H}{\nu}, \quad (4)$$

where  $\nu$  is the kinematic viscosity and  $U_{\text{up,down}}$  is the maximum of the profile along  $x$  of vertical velocity in the plane at mid-height.

At first glance, the Reynolds number is quite similar across various experiments in the literature, regardless of discrepancies in the Nusselt number. Rough or smooth, ultimate regime or not, Rayleigh number ranging from  $10^{10}$  to  $10^{13}$ , Prandtl number between 0.8 and 14, their Reynolds number seems to collapse with a scaling  $Re \sim Ra^{1/2} Pr^{-0.7}$ , see Figure 4. However, there are some small differences, and these may become more significant for quantities that scale with a power of the Reynolds number. In particular, the Reynolds number in the rough cell using fluorocarbon is larger than in the smooth case, and additionally is asymmetrical (velocity is larger near the rough plate). This Reynolds number enhancement triggered by roughness was not visible in our previous measurements using PIV in water

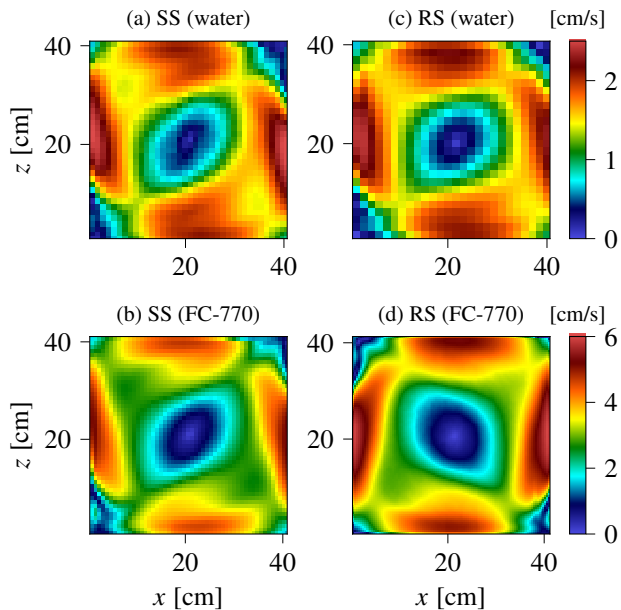


FIG. 3. Mean velocity maps computed from the Shadowgraph recording in SS (a, b) and RS (c, d). (a) SS Water  $Ra = 6.3 \times 10^{10}$ ,  $Re = 1.6 \times 10^4$ ,  $v_{\max} = 2.5$  cm/s; (b) SS FC-770  $Ra = 1.7 \times 10^{12}$ ,  $Re = 3.3 \times 10^4$ ,  $v_{\max} = 5.2$  cm/s; (c) RS Water  $Ra = 5.6 \times 10^{10}$ ,  $Re = 1.4 \times 10^4$ ,  $v_{\max} = 2.4$  cm/s; (d) RS FC-770  $Ra = 1.6 \times 10^{12}$ ,  $Re = 4.0 \times 10^4$ ,  $v_{\max} = 5.9$  cm/s.

at lower Rayleigh numbers [22]. Indeed, the new data obtained in fluorocarbon is further from the threshold where roughness-enhanced heat-transfer is triggered than the rough cell using water. While the previous measurements in water was in Regime II (as defined by Xie & Xia [18]), where the kinematic boundary layer remains larger than the roughness elements, the fluorocarbon cell is in Regime III, where both thermal and kinetic boundary layers are smaller than the roughness height.

One interesting quantity is the friction coefficient,

$$\frac{RaNu}{Re^3 Pr^2}, \quad (5)$$

which was used by Chavanne, *et al.* as an indicator of the transition to turbulence in the boundary layers [19], and can alternatively be interpreted as proportional to the ratio between the kinetic energy dissipation rate  $\epsilon$  and the bulk energy dissipation rate  $\epsilon_{u,bulk}$  [23],

$$\epsilon = \frac{\nu^3}{H^4} (Nu - 1) Ra Pr^{-2}, \quad (6)$$

$$\epsilon_{u,bulk} \propto \frac{\nu^3}{H^4} Re^3. \quad (7)$$

In the range of parameters explored in this work, we evidence a transition at a critical Reynolds number,

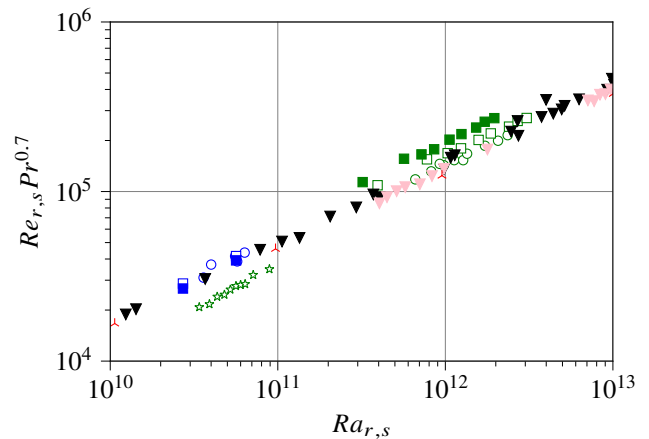


FIG. 4. Reynolds number measurements in water (blue) and FC-770 (green), in RS (squares) and SS (circles) cells. Open squares are smooth half-cell. Full squares are rough half-cell. Green stars are the  $\Gamma = 2$  cell. For comparison: Grenoble data [19] (black triangles), Göttingen data [20] (pink triangles), Oregon data [21] (red 3-branched stars).

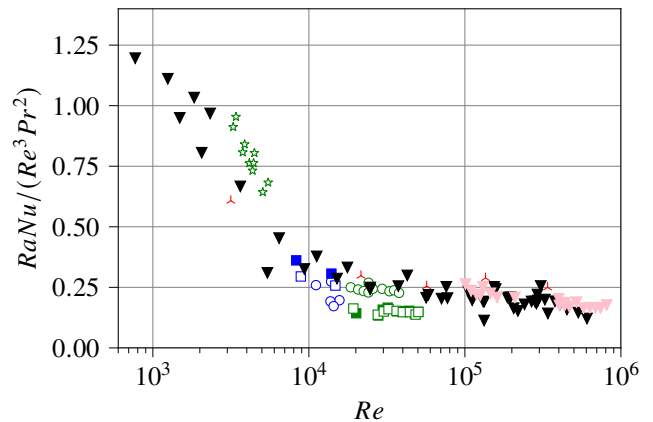


FIG. 5. Friction coefficient for all data points (same colors as Figure 4). The heat flux,  $RaNu$  collapses for all data with  $RaNu \sim 0.2 Re^3 Pr^2$  (with this definition of the Reynolds number).

$Re_c \approx 10^4$ . Beyond this transition, the friction coefficient no longer depends on the Reynolds number, or only very weakly, see Figure 5. Therefore, we get a relationship between the dimensionless heat-flux,  $RaNu$ , and the Reynolds and Prandtl numbers, where

$$RaNu = \frac{g\alpha H^4}{\mu\lambda^2} \dot{Q}, \quad (8)$$

where  $g$  the acceleration of gravity,  $\alpha$  the thermal expansion coefficient,  $H$  the height of the cell,  $\mu$  the dynamical viscosity,  $\lambda$  the thermal conductivity, and  $\dot{Q}$  the heat-flux. The phenomenological relationship is,

$$RaNu \approx 0.2 Re^3 Pr^2. \quad (9)$$

However, this result does not allow to directly infer

whether the kinetic energy dissipation rate is dominated by the bulk energy dissipation rate, or how much dissipation in the boundary layers still contributes, because of prefactors stemming from the non-unique definition for the Reynolds number and of the turbulent dissipation.

It is remarkable that this relationship, Eq. 9, holds for the Grenoble data which evidence a transition to the ultimate regime, as well as data which does not evidence such transition, and also in the case of rough cells in which  $Nu \sim Ra^{1/2}$ , as well as smooth cells with a classical scaling. This shows that whatever changes are triggered by either the roughness or the transition to the ultimate regime are entirely taken into account in the Reynolds number. While it may seem at first glance that the Reynolds number is only a function of  $Ra$  and  $Pr$ , it really is not. Multiple flows are possible at a given Rayleigh number [9, 24], and it is therefore elusive to try to determine a threshold in terms of Rayleigh numbers for such transitions. The universal scaling for the heat-flux, Eq. 9, evidenced in this work, has to be taken into account in tentative theoretical models of turbulent thermal convection.

#### ACKNOWLEDGEMENTS

The authors are thankful to Marc Moulin and his team at the mechanical workshop for the design and machining of the experimental apparatus. This work was funded by ANR-18-CE30-0007-01 JCJC ‘‘CryoGrad’’ project, and benefited from the resources of the PSMN computing center in Lyon.

---

\* julien.salort@ens-lyon.fr

- [1] F. Chillà and J. Schumacher, New perspectives in turbulent Rayleigh-Bénard convection, *Eur. Phys. J. E* **35**, 58 (2012).
- [2] R. J. A. M. Stevens, E. P. van der Poel, S. Grossmann, and D. Lohse, The unifying theory of scaling in thermal convection: the updated prefactors, *J. Fluid Mech.* **730**, 295 (2013).
- [3] L.-A. Couston and M. Siegert, Dynamic flows create potentially habitable conditions in Antarctic subglacial lakes, *Sci. Adv.* **7**, eabc3972 (2021).
- [4] R. H. Kraichnan, Turbulent thermal convection at arbitrary Prandtl number, *Phys. Fluids* **5**, 1374 (1962).
- [5] X. Chavanne, F. Chillà, B. Castaing, B. Hébral, B. Chabaud, and J. Chaussy, Observation of the ultimate regime in Rayleigh-Bénard convection, *Phys. Rev. Lett.* **79**, 3648 (1997).
- [6] J. J. Niemela and K. R. Sreenivasan, Confined turbulent convection, *J. Fluid Mech.* **481**, 355 (2003).
- [7] X. He, D. Funfschilling, E. Bodenschatz, and G. Ahlers, Heat transport by turbulent Rayleigh-Bénard convection for  $Pr \simeq 0.8$  and  $4 \times 10^{11} < Ra < 2 \times 10^{14}$ : ultimate-state transition for aspect ratio  $\gamma = 1.00$ , *New J. Phys.* **14**, 063030 (2012).
- [8] J. J. Niemela, L. Skrbek, K. R. Sreenivasan, and R. J. Donnelly, Turbulent convection at very high Rayleigh numbers, *Nature* **404**, 837 (2000).
- [9] P.-E. Roche, F. Gauthier, R. Kaiser, and J. Salort, On the triggering of the ultimate regime of convection, *New J. Phys.* **12**, 085014 (2010).
- [10] P.-E. Roche, The ultimate state of convection: a unifying picture of very high Rayleigh numbers experiments, *New J. Phys.* **22**, 073056 (2020).
- [11] G. Ahlers, E. Bodenschatz, R. Hartmann, X. He, D. Lohse, P. Reiter, R. J. A. M. Stevens, R. Verzicco, M. Wedi, S. Weiss, X. Zhang, L. Zvirner, and O. Shishkina, Aspect ratio dependence of Heat transfer in a Cylindrical Rayleigh-Bénard cell, *Phys. Rev. Lett.* **128**, 084501 (2022).
- [12] D. Lohse and O. Shishkina, Ultimate turbulent thermal convection, *Phys. Today* **76**, 26 (2023).
- [13] L. Méthivier, R. Braun, F. Chillà, and J. Salort, Turbulent transition in Rayleigh-Bénard convection with fluorocarbon, *EPL* **136**, 10003 (2021).
- [14] M. Belkadi, L. Guislain, A. Sergent, B. Podvin, F. Chillà, and J. Salort, Experimental and numerical shadowgraph in turbulent Rayleigh-Bénard convection with a rough boundary: investigation of plumes, *J. Fluid Mech.* **895**, A7 (2020).
- [15] J.-C. Tisserand, M. Creyssels, Y. Gasteuil, H. Pabiau, M. Gibert, B. Castaing, and F. Chillà, Comparison between rough and smooth plates within the same Rayleigh-Bénard cell, *Phys. Fluids* **23**, 015105 (2011).
- [16] E. Rusaouen, O. Liot, J. Salort, B. Castaing, and F. Chillà, Thermal transfer in Rayleigh-Bénard cell with smooth or rough boundaries, *J. Fluid Mech.* **837**, 443 (2018).
- [17] J. Salort, O. Liot, E. Rusaouen, F. Seychelles, J.-C. Tisserand, M. Creyssels, B. Castaing, and F. Chillà, Thermal boundary layer near roughnesses in turbulent Rayleigh-Bénard convection: flow structure and multi-stability, *Phys. Fluids* **26**, 015112 (2014).
- [18] Y.-C. Xie and K.-Q. Xia, Turbulent thermal convection over rough plates with varying roughness geometries, *J. Fluid Mech.* **825**, 573 (2017).
- [19] X. Chavanne, F. Chillà, B. Chabaud, B. Castaing, and B. Hébral, Turbulent Rayleigh-Bénard convection in gaseous and liquid he, *Phys. fluids* **13**, 1300 (2001).
- [20] X. He, D. P. M. van Gils, E. Bodenschatz, and G. Ahlers, Reynolds numbers and the elliptic approximation near the ultimate state of turbulent Rayleigh-Bénard convection, *New J. Phys.* **17**, 063028 (2015).
- [21] J. J. Niemela, L. Skrbek, K. R. Sreenivasan, and R. J. Donnelly, The wind in confined thermal convection, *Journal of Fluid Mechanics* **449**, 169 (2001).
- [22] O. Liot, Q. Ehlinger, E. Rusaouën, T. Coudarchet, J. Salort, and F. Chillà, Velocity fluctuations and boundary layer structure in a rough Rayleigh-Bénard cell filled with water, *Phys. Rev. Fluids* **2**, 044605 (2017).
- [23] S. Grossmann and D. Lohse, Scaling in thermal convection: a unifying theory, *J. Fluid Mech.* **407**, 27 (2000).
- [24] P.-E. Roche, *Convection thermique turbulente en cellule de Rayleigh-Bénard cryogénique*, Ph.D. thesis, Université Joseph-Fourier (2001).